

# Robotic Inventorying and Localization of RFID Tags, Exploiting Phase-Fingerprinting

Stavroula Siachalou\*, Spyros Megalou\*, Anastasios Tzitzis\*, Emmanouil Tsardoulidas\*, Aggelos Bletsas†, John Sahalos‡, Traianos Yioultsis\*, Antonis G. Dimitriou\*

\*School of Electrical and Computer Engineering, Aristotle University of Thessaloniki Thessaloniki, Greece

† School of Electrical and Computer Engineering, Technical University of Crete, Chania, Greece

‡ School of Electrical and Computer Engineering, University of Nicosia, Nicosia, Cyprus  
antodimi@ece.auth.gr

**Abstract**—In this paper we investigate the performance of phase-based fingerprinting for the localization of RFID-tagged items in warehouses and large retail stores, by deploying ground and aerial RFID-equipped robots. The measured phases of the target RFID tags, collected along a given robot’s trajectory, are compared to the corresponding phase-measurements of reference RFID tags; i.e. tags placed at known locations. The advantage of the method is that it doesn’t need to estimate the robot’s trajectory, since estimation is carried out by comparing phase measurements collected at neighboring time-intervals. This is of paramount importance for an RFID equipped drone, destined to fly indoors, since its weight should be kept as low as possible, in order to constrain its diameter correspondingly small. The phase measurements are initially unwrapped and then fingerprinting is applied. We compare the phase-fingerprinting with RSSI based fingerprinting. Phase-fingerprinting is significantly more accurate, because of the shape of the phase-function, which is typically U-shaped, with its minimum, measured at the point of the trajectory, when the robot-tag distance is minimised. Experimental accuracy of 15cm is typically achieved, depending on the density of the reference tags’ grid.

**Index Terms**—RFID, localization, drone, robot, fingerprinting, phase

## I. INTRODUCTION

This work is part of the project ”RELIEF”, [1], where we focus on automated 24/7 inventorying, exploiting robots and drones. Part of our work has been recently presented in [2], [3]. We target cm-accuracy localization of the stock. Solutions including fixed readers and antennas are prohibitive for large areas, due to the associated cost, while static installations may result in constant maxima and minima of the field, due to constructive or destructive interference patterns ([4]). In contrast, the proposed method guarantees 24-hour monitoring by using a single RFID-equipped robot (Fig. 1) or drone (Fig. 2), capable of moving or flying around the target area. Optical sensors can be placed on terrestrial robots to perform mapping and localization of the robot’s position. However, ground robots can’t efficiently scan regions of higher elevation. In such cases warehouse RFID drones can be used. To ensure

longer time-of-flight of the drone, which is affected by the battery’s capacity and the total weight of the load, we avoid heavy-weight sensing-equipment related to mapping of the environment and accurately locating the drone’s position. Instead, due to the lack of such equipment, we assume that the actual location of the robot/drone is not known, while the drone only carries equipment to ensure a secure flight in the target area.

Fingerprinting is a family of methods that doesn’t need to know the location of the robot. Localization of the target tags (and the attached objects) is sought by deploying reference or anchor tags; i.e. tags placed at known locations. RFID reference tags are placed in known positions creating a grid around the target tags. The RFID reader on the robot collects data as it moves around the target area. Depending on the number of considered tags one can adjust the robot’s speed. The advantage of this method is its cost minimization, as neither extra readers nor optical sensors are used for the robot’s localization. Instead a dense grid of low-cost passive RFID reference tags will improve the accuracy of locating the target tags.

Prior art concerning localization of RFID tags, focuses on utilizing *i*) the phase of the modulated backscattered signal or, *ii*) the Received Signal Strength Information (RSSI) from each tag to pinpoint them at a predicted position. The majority of localization techniques need to know the consecutive positions of the reader to locate the tags. We can classify these methods into direction-finding [10], [11], Synthetic Aperture Radar methods (SAR) [12]- [15], methods based on Conditional probability [5]- [9] and distance-estimation methods [16]. Great accuracy can be achieved using SAR methods. However the robot’s/reader’s position must be known exactly. Precise estimation of the robot’s path is not an easy task especially when the robot uses SLAM techniques [21], to perform mapping as well.

In this paper we focus on Fingerprinting methods and with respect to prior art [18]- [20] we compare the phase-fingerprinting with RSSI based fingerprinting, recently presented in [2].

This research has been co-financed by the European Union and Greek national funds through the Operational Program Competitiveness, Entrepreneurship and Innovation, under the call RESEARCH CREATE INNOVATE (project code:T1EDK-03032).

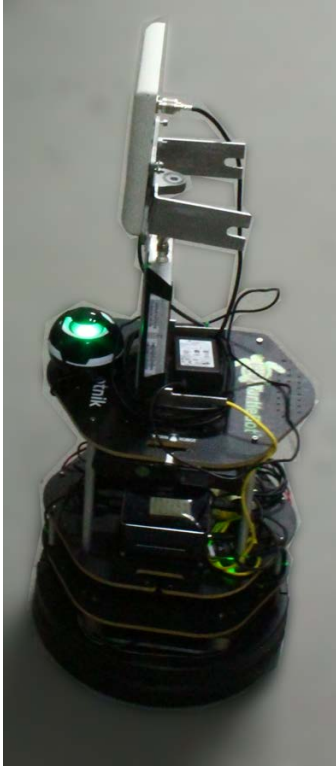


Fig. 1. Prototype robot, including UHF RFID equipment.



Fig. 2. Prototype drone for UHF RFID inventorying.

## II. PROBLEM FORMULATION

### A. Notation

In this section we present the formulation and notation that will be used in the rest of the paper. Let  $(M, U, N)$  represent a region under consideration with reference tag set  $M$ , tracked tag set  $U$  and antenna set  $N$ . In the moving robot/drone problem, each element in antenna set  $N$  corresponds to a specific antenna (the robot could include multiple) and a small

time interval (for which the movement of the robot is much smaller than the wavelength). The  $|M|$  RFID tags are placed at known locations around the region, where  $|U|$  unknown tags are "tracked". Let  $X_i^j$  the measurements collected from antenna  $i \in N$ , of tracked tag  $j \in U$  and  $R_i^l$  the measurements from antenna  $i \in N$ , of reference tag  $l \in M$ . Denote  $\mathbf{X}^j = (X_1^j, X_2^j, \dots, X_{|N|}^j)$  the set of measurements of tracked tag  $j \in U$  by the antenna set  $N$  and  $R^l = (R_1^l, R_2^l, \dots, R_{|N|}^l)$ , the corresponding collection of measurements of reference tag  $l \in M$ , from the same antenna set  $N$ . We create an indicator function equal to one when antenna  $i \in N$  identifies the pair  $(j, l)$  simultaneously, otherwise equal to zero,

$$I_i(j, l) = \begin{cases} 1 & \text{if } (j, l) \text{ are both identified from antenna } i \\ 0 & \text{else} \end{cases} \quad (1)$$

The number of common measurements of each pair  $(j, l)$  is

$$C_l^j = \sum_{i=1}^{|N|} I_i(j, l) \quad (2)$$

For each pair of tracked-reference tag  $(j, l)$ , we define the following distance-"resemblance" metric:

$$D_l^j = \begin{cases} \sqrt{\sum_{i=1}^{|N|} I_i(j, l) (X_i^j - R_i^l)^2} & \text{if } C_l^j > 0 \\ \infty & \text{if } C_l^j = 0 \end{cases} \quad (3)$$

For each tracked tag  $j \in U$ , we create a distance-resemblance vector:

$$\mathbf{D}^j = (D_1^j, D_2^j, \dots, D_{|M|}^j) \quad (4)$$

and the corresponding common measurements counter vector:

$$\mathbf{C}^j = (C_1^j, C_2^j, \dots, C_{|M|}^j) \quad (5)$$

When a tracked tag  $j$  is physically close to a reference tag, it is expected to have many common measurements. The corresponding element in vector  $\mathbf{C}$ , defined in (5), will be large. On the contrary, distant tags will have small or zero values in (5). We define the mean of common measurements **for each** tracked tag:

$$C_{mean}^j = \frac{\sum_{l=1}^{|M|} C_l^j}{a}, \forall j \in U \quad (6)$$

where  $a$  is the number of non-zero elements of  $\mathbf{C}^j$ . Then, in order to discard reference tags with few common measurements with the tracked tag, we define a threshold  $L^j$  to be proportional to the above mean of each tag  $j$  by an optimization parameter  $g$ :

$$L^j = gC_{mean}^j, \quad (7)$$

Then, we modify (3), in order to discard reference tags with few common measurements with the specific tracked tag:

$$D_l^{j'} = \begin{cases} D_l^j & \text{if } C_l^j > L^j \\ \infty & \text{else} \end{cases} \quad (8)$$

Vector in (4) is updated accordingly:

$$\mathbf{D}^j = (D_1^j, D_2^j, \dots, D_{|M|}^j) \quad (9)$$

The smallest element in (9) represents the reference tag, for which the measured values best fitted the corresponding measured values of the tracked tag, while enough common measurements are collected. Hence, we expect the actual location of the tracked tag to be "closer" to that reference tag. Furthermore, the "resemblance" vector can be used as a distance indicator from each reference tag, thus "weighting" the distance of the "target" tag from each reference tag. Since the smallest elements in (9) are more significant, the corresponding resemblance metric should be inverted. Let  $v$  represent an optimization parameter and  $\mathbf{H}^j$  is a vector which contains only the  $k$  nearest neighbors of vector  $\mathbf{D}^j$ .

$$\mathbf{H}^j = \text{kSmallestElements}(\mathbf{D}^j) \quad (10)$$

To estimate the coordinates of target tag  $j \in U$  we need the following two equations:

$$(x^j, y^j) = \sum_{i=1}^k w_i * (x^i, y^i) \quad (11)$$

$$w_i = \frac{1/(H_i^j)^v}{\sum_{i=1}^k 1/(H_i^j)^v}, i = 1, 2, \dots, k \quad (12)$$

### B. Phase Unwrapping and Fingerprinting

In [2], an RSSI-based Fingerprinting Localization algorithm has been introduced. In [3] the authors presented the Phase ReLock method for RFID localization, which solves by standard optimization methods a problem, originating from Synthetic Aperture Radar theory, by phase unwrapping each tag's sequence of measurements and changing the optimization function. In this paper we exploit advantages of the two techniques; i) we use the unwrapped sequence of samples collected by the robot instead of the backscattered power, expecting to represent a much better estimator, due to the monotony of the measured samples (not including local minima and maxima) and the immunity of the phase measurements to blocking of the tag or small detuning in the vicinity of different materials, ii) the method does not depend on the locations of the robot/drone; which is necessary for Phase ReLock. The phase data collected from a tag, before and after the unwrapping procedure are shown in Fig. 3.

The proposed method consists of two main steps. In the first step phase measurements of each tag are collected and unwrapped. In the second step the unwrapped phase is used to find the location of the tracked tags with the fingerprinting technique. Depending on the robots' speed, a time frame  $dt$  is assumed, within which a single antenna location  $i$  is mapped.

### C. Exploitation of the reference tag

The reference tags are placed in known positions and are also treated as unknown tags in order to estimate the mean error, by changing optimization parameters of the algorithm, e.g. threshold  $g$  of (7). Now assume a tag  $j$  is measured  $s$

times from moving antenna. For each time  $t_i, i \in (1, 2, \dots, s)$  we create a time frame  $dt$  centered around  $t_i$ . In this time frame some reference tags are measured simultaneously with tag  $j$ . The proposed method keeps phase measurements of each pair  $(j, l), l \in M$ . In case a reference tag  $l$  is read more than once in a specific time frame, than the method keeps the phase sample which occurred closer in time to the tracked tag  $j$ , in the specific time interval.

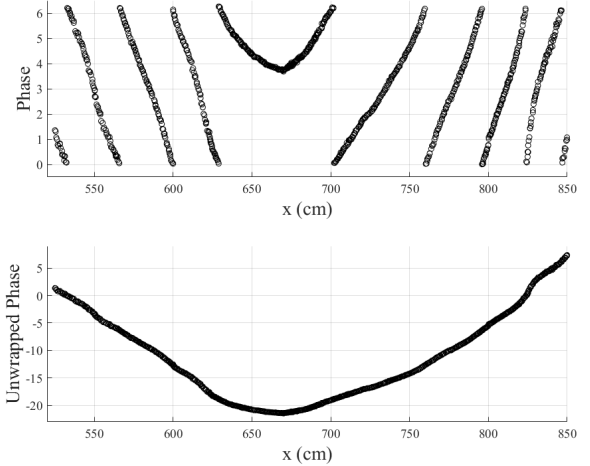


Fig. 3. Wrapped vs Unwrapped Phase data from the same tag in respect to robot's displacement.

## III. EXPERIMENTS

Even though the proposed fingerprinting techniques is ideal for the lightweight drone, the experiments were conducted using the ground robot of Fig. 1. The experiments were carried out along a straight corridor, where 87 RFID tags are placed on a 10m-long millimetre-paper on top of a bench. 45 are used as reference tags, 42 are the tracked tags, while the robot is equipped with one reader and one antenna, as demonstrated in Fig. 4. The experiments were repeated several times and the robot moved at different speeds (5cm/sec, 10cm/sec and 20cm/sec) and traversed different traces, as depicted in Fig. 5. The paths shown in Fig. 5 were estimated by the SLAM algorithm embedded in the robot; however this information is not used by the fingerprinting algorithm. Two more slalom paths, not shown in Fig. 5 for convenience, were carried out and the corresponding results are given in Tables II, III as (S1, S2). In some experiments, part of the tags (reference and tracked) were blocked by dielectrics, as demonstrated in Fig. 4. The purpose is to show the vulnerability vs. the immunity of the RSSI-fingerprinting method vs. the phase-fingerprinting method respectively. Results with obstacles are presented in Table II as OB1, OB2, OB3 depending on the used speed and the distance from the bench.

### A. Phase over RSSI; A superior indicator.

As the robot moves along any path, it continuously interrogates all RFID tags within range and stores the ID, the RSSI,

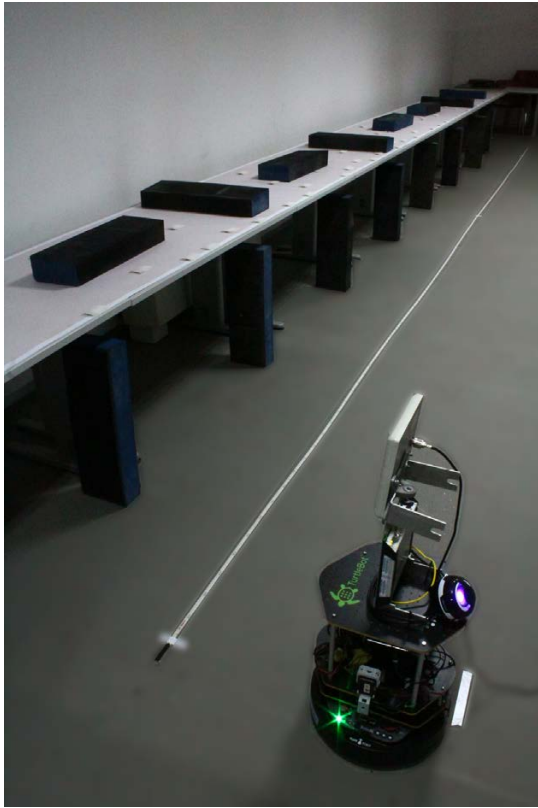


Fig. 4. Estimated trajectories of the robot for different experiments, based on SLAM.

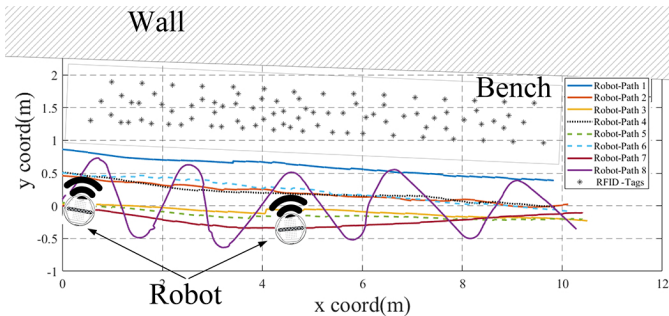


Fig. 5. Estimated trajectories of the robot for different experiments, based on SLAM.

the phase information with a time-stamp for each sample. As a characteristic example of the stored data, consider the plot of Fig. 6, where both the unwrapped phase (top) and the RSSI power (bottom) data for a specific tag are demonstrated as the robot moves on a straight path along the x-axis of the room. The x-axis of Fig. 6 corresponds to the x-coordinate of the robot; we could have plotted the time-data instead.

As discussed earlier, the measured phase of each tag decreases as the robot approaches the tag and increases as the robot gets away from the tag (U-shaped curve). In between there is a single minimum of the curve that corresponds to the time (or x-coordinate in Fig. 6), when the robot-tag distance was minimized (at this point the tag is located along a straight

line that intersects perpendicularly the trace of the robot). Now consider the corresponding RSSI measurements also shown in Fig. 6, where one might expect the RSSI to be maximized at the point when the phase was minimized (675cm). However, the power is vulnerable to multipath. Therefore, the curve suffers from multiple maxima and the biggest one is recorded at 740cm.

Now consider that a tracked tag is located at 740cm, as demonstrated in Fig. 7. The corresponding measurements collected by the robot are shown along the same axes as those of the reference tag. Notice that the new phase curve follows a similar pattern as that of the reference tag, only shifted to the right by 65cm, whereas the RSSI pattern of the tracked tag now suffers from less fading and experiences its maximum at the expected position at 740cm. The phase differences between the reference and the tracked tag, used by the fingerprinting method in (3) correspond well to the actual (physical) distance between the two tags on the bench. However, due to fading, the RSSI differences between the two tags are small; therefore, the RSSI-fingerprinting algorithm decides that the location of the tracked tag coincides with that of the reference tag.

The second advantage of the phase sequence over the RSSI sequence is its immunity to typical effects, strongly affecting the power of the backscattered signal. The accuracy of the fingerprinting method is based on the resemblance of the electromagnetic environment of the reference tags with the target tags. However, power is more sensitive to such effects: namely power is affected by blocking (a phase sequence isn't), power is affected by neighboring materials (detuning of antenna), power is affected by the antenna's radiation pattern (phase isn't).

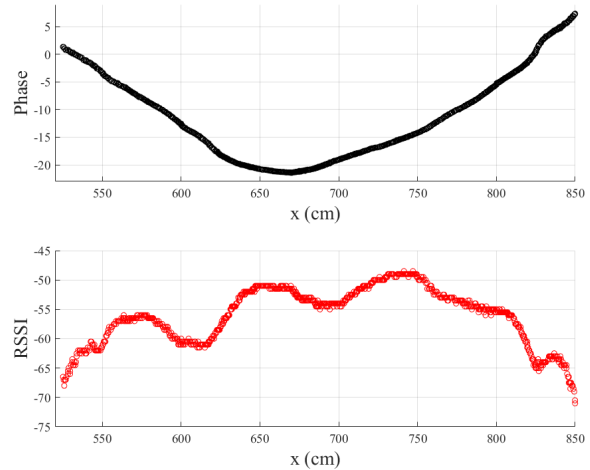


Fig. 6. Phase vs RSSI data collected from the same tag in respect to robot's displacement.

### B. Variability of the accuracy vs. optimization parameters of the fingerprinting method

We investigate how the mean estimation error changes with respect to the optimization parameters  $g$ ,  $k$ ,  $u$  along the

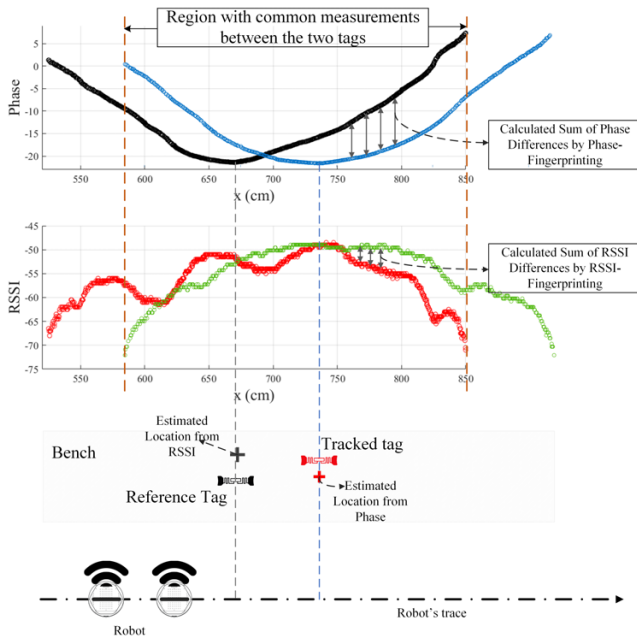


Fig. 7. Phase vs RSSI analysis of error.

experiments. The localization error for each tag is estimated by calculating the Euclidean distance between the tag's estimated position  $(x_{est}, y_{est})$  and tag's real position  $(x_{real}, y_{real})$ . Results showed that for each different path or speed of the robot, a different selection of the three optimization parameters minimized the localization error, likewise the results in [2]. However, in contrast to RSSI-fingerprinting, the variability of the error for different selection of the parameters is small. Such characteristic results are demonstrated in Figs. 8-10. In these representative results, we have changed  $g$  from 0.8 to 1.6 and  $k$  from 4 to 6. The variability of the mean error is within 1cm. For the corresponding values, the RSSI-fingerprinting error varies within 10cm. The error and the standard deviation from all experiments are summarized in Tables I and II where they are compared against RSSI-fingerprinting results for the same experiments. As expected, phase-fingerprinting outperforms RSSI, achieving a mean-error of only 15.5cm vs. 23.83cm respectively for straight paths. Results in Table II present mean estimation error of 18.9cm and 24.4cm when the robot uses a slalom path (S1,S2) and when obstacles are placed on top of the bench, for the compared methods. In all cases, the corresponding error is calculated by the reference tags as well (they are treated as target tags). This error follows reasonably well the corresponding error of the actual tags and is used for real-time performance assessment in actual environments.

Additional experiments were held by decreasing the number of reference tags to  $|M| = 25$ . Results in Table III compare the mean estimation error of tracked tags for  $|M| = 45$  (All) and  $|M| = 25$  (few). A narrow grid of reference tags, for either the RSSI or the phase-fingerprinting algorithm, leads to an increase of the mean errors of both methods.

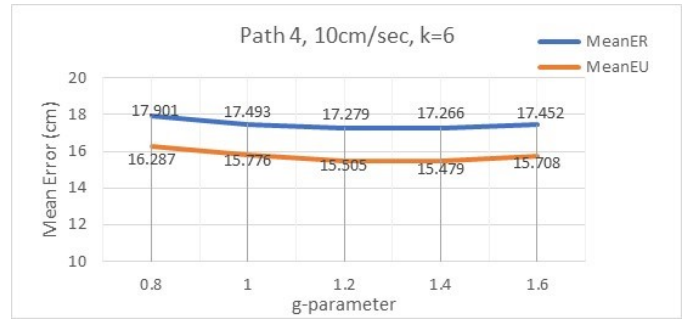


Fig. 8. Mean Error in cm of Reference Tags (MeanER) and Tracked Tags (MeanEU) from path 4, k=6 and  $|M| = 45$ .

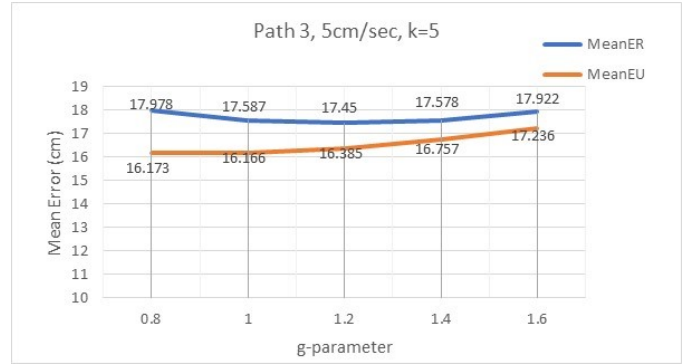


Fig. 9. Mean Error in cm of Reference Tags (MeanER) and Tracked Tags (MeanEU) from path 3 and k=5.

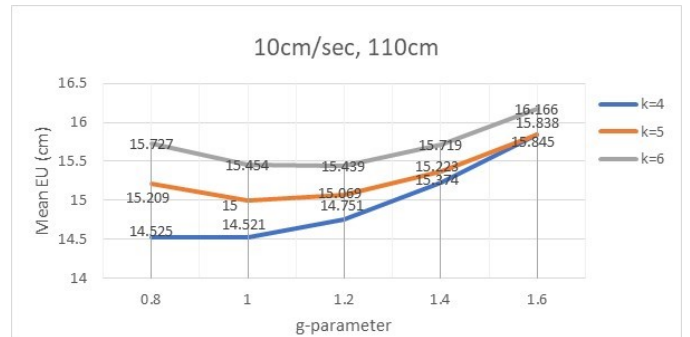


Fig. 10. Mean Error in cm of Tracked Tags (MeanEU) for path 5.

TABLE I  
PHASE VS RSSI EXPERIMENTAL RESULTS FOR STRAIGHT PATHS

Path	Speed cm/sec	Phase Mean Error Ref. (cm)	Phase Mean Error Target (cm)	Phase Std Error (cm)	RSSI Mean Error Ref. (cm)	RSSI Mean Error Target (cm)	RSSI Std Error (cm)
1	5	20.47	17.81	9.9	34.668	28.76	20.39
2	5	17.67	15.19	9.76	25.21	19.46	9.89
3	5	14.65	15.93	10.24	28.665	23.97	14.73
4	10	14.65	15.33	9.06	26.568	19.13	9.26
5	10	14.49	14.52	9.35	27.919	26.83	17.97
6	20	14.5	14.70	8.25	23.335	19.49	10.70
7	20	15.96	15.05	9.61	26.381	29.22	15.46

TABLE II  
PHASE VS RSSI EXPERIMENTAL RESULTS FOR SLALOM PATHS AND PATHS WITH OBSTACLES

Path	Speed cm/sec	Phase Mean Error Ref. (cm)	Phase Mean Error Target (cm)	Phase Std (cm)	RSSI Mean Error Ref. (cm)	RSSI Mean Error Target (cm)	RSSI Std (cm)
S1	5	23	20.25	14.57	21.725	21.37	13.07
S2	10	24.38	20.29	12.41	23.834	24.45	13.78
OB1	5	23.06	19.261	15.36	42.95	26.61	19.93
OB2	10	21.5	17.729	13.836	35.36	23.4	15.37
OB3	20	20.94	17.43	16.22	36.31	26.46	21.85

TABLE III  
PHASE VS RSSI EXPERIMENTAL RESULTS OF TRACKED TAGS FOR ALL AND FEW REFERENCE TAGS

Path	Speed cm/sec	Phase	Phase	RSSI	RSSI
		Mean Error $ M  = 45$ (cm)	Mean Error $ M  = 25$ (cm)	Mean Error $ M  = 45$ (cm)	Mean Error $ M  = 25$ (cm)
1	5	17.81	24.155	28.76	31.285
2	5	15.19	22.55	19.46	24.203
3	5	15.93	22.5	23.97	28.073
4	10	15.33	22.68	19.13	25.761
5	10	14.52	22.73	26.83	30.729
6	20	14.7	19.3	19.49	24.704
7	20	15.05	20.68	29.22	30.257
S1	5	20.25	20.81	21.37	26.78
S2	10	20.29	26.21	24.45	29.679

#### IV. CONCLUSION

In this paper we have presented a phase fingerprinting localization method for robot/drone inventorying, which is designed to be deployed, when the robot/drone's trace cannot be accurately estimated. The proposed method outperforms the RSSI fingerprinting, recently presented in [2], thanks to the immunity of the phase-measured sequence of data to multipath fading and coupling effects with the environment. The proposed method can be applied to lightweight drones designed to fly indoors and outdoors without the necessary sensor-equipment for localization of their own position. Experimental mean error of 15cm-22cm was maintained in all 12 experiments, where different setups were evaluated.

#### REFERENCES

[1] RELIEF project, "http://relief.web.auth.gr/", last accessed on June 5 2019.

[2] S. Megalou, A. Tzitzis, S. Siachalou, T. Yioultsis, J. Sahalos, E. Tsardoulas, A. Filotheou, A. Symeonidis, L. Petrou, A. Bletsas, A. G. Dimitriou, "Fingerprinting Localization of RFID tags with Real-Time Performance-Assessment, using a Moving Robot," 13th European Conference on Antennas and Propagation, Krakow, Poland, March 2019.

[3] A. Tzitzis, S. Megalou, S. Siachalou, T. Yioultsis, A. Kehagias, E. Tsardoulas, A. Filotheou, A. Symeonidis, L. Petrou, A. G. Dimitriou, "Phase ReLock - Localization of RFID Tags by a Moving Robot," 13th European Conference on Antennas and Propagation, Krakow, Poland, March 2019.

[4] T. Faseth, M. Winkler, H. Arthaber, and G. Magerl, "The Influence of Multipath Propagation on Phasebased Narrowband Positioning Principles in UHF RFID," 2011 IEEEAPS Topical Conference on Antennas and Propagation in Wireless Communications (APWC), Torino, Italy, 2011.

[5] S. Siachalou, A. Bletsas, J. N. Sahalos and A. G. Dimitriou, "RSSIbased Maximum Likelihood Localization of Passive RFID Tags Using a Mobile Cart," IEEE Wireless Power Transfer Conference (WPTC), Aveiro, Portugal, 2016.

[6] S. Subedi, E. Pauls, and Y. D. Zhang, "Accurate Localization and Tracking of a Passive RFID Reader based on RSSI Measurements," IEEE Journal of Radio Frequency Identification, vol. 1, no. 2, pp. 144-54, 2017.

[7] J. Zhang, Y. Lyu, J. Patton, S.C. G. Periaswamy, and T. Roppel, "BFVP: A Probabilistic UHF RFID Tag Localization Algorithm Using Bayesian Filter and a Variable Power RFID Model," IEEE Transactions on Industrial Electronics, vol. 65, no. 10, pp. 8250-8259, 2018.

[8] F. Martinelli, "A Robot Localization System Combining RSSI and Phase Shift in UHF RFID Signals," IEEE Transactions on Control Systems Technology, vol. 23, no. 5, pp. 1782-1796, 2015.

[9] P. Yang, and W. Wu, "Efficient Particle Filter Localization Algorithm in Dense Passive RFID Tag Environment," IEEE Transactions on Industrial Electronics, vol. 61, no. 10, pp. 5641-5651, 2014.

[10] J. Zhou, H. Zhang, and L. Mo, "Twodimension Localization of Passive RFID Tags Using AOA Estimation," 2011 IEEE Instrumentation and Measurement Technology Conference (I2MTC), Binjiang, China, 2011.

[11] S. Azzouzi, M. Cremer, U. Dettmar, R. Kronberger, and T. Knie, "New Measurement Results for the Localization of UHF RFID Transponders Using an Angle of Arrival (AoA) Approach," 2011 IEEE International Conference on RFID, Orlando (Fl), 2011.

[12] A. Motroni, P. Nepa, V. Magnago, A. Buffi, B. Tellini, D. Fontanelli, and D. Macii, "SAR-Based Indoor Localization of UHF-RFID Tags via Mobile Robot," 2018 International Conference on Indoor Positioning and Indoor Navigation (IPIN), Nantes, France, 2018.

[13] R. Miesen, F. Kirsch, and M. Vossiek, "Holographic Localization of Passive UHF RFID Transponders," 2011 IEEE International Conference on RFID, Orlando, Florida, 2011.

[14] L. Yang, Y. Chen, X. Y. Li, C. Xiao, M. Li, and Y. Liu, "Tagoram: Realtime Tracking of Mobile Rfid Tags to High Precision Using Cots Devices," In Proceedings of the 20th annual international conference on Mobile computing and networking, pp. 237-248, 2014.

[15] L. Shangguan, and K. Jamieson, "The Design and Implementation of a Mobile Rfid Tag Sorting Robot," In Proceedings of the 14th Annual International Conference on Mobile Systems, Applications, and Services, pp. 31-42, 2016.

[16] Y. Ma, N. Selby, and F. Adib, "Minding the Billions: UltraWideband Localization for Deployed RFID Tags," MobiCom 2017, 23rd Annual Conference on Mobile Computing and Networking, Utah, USA, 2017.

[17] P. V. Nikitin, R. Martinez, S. Ramamurthy, H. Leland, G. Spiess, and K. V. S. Rao, "Phase Based Spatial Identification of UHF RFID Tags," 2010 IEEE International Conference on RFID, Orlando, Florida, 2010.

[18] J. Trogh, D. Plets, L. Martens, W. Joseph, "Advanced Real-Time Indoor Tracking Based on the Viterbi Algorithm and Semantic Data," Location-Related Challenges and Strategies in Wireless Sensor Networks, vol. 11, no. 10, 2015.

[19] L. M. Ni, and Y. Liu, "LANDMARC: Indoor Location Sensing Using Active RFID," Wireless Networks, vol. 10, no. 6, pp. 701-710, 2004.

[20] J. Wang, and D. Katabi, "Dude, Where's my Card?: RFID Positioning that Works with Multipath and Nonline of Sight," Proceedings of the ACM SIGCOMM 2013 conference on SIGCOMM, pp. 51-62, Hong kong, China, 2013.

[21] C. Cadena, L. Carlone, H. Carillo, Y. Latif, D. Scaramuzza, J. Neira, I. Reid, and J. J. Leonard, "Past, Present, and Future of Simultaneous Localization and Mapping: Toward the Robust-Perception Age," IEEE Transactions on Robotics, vol. 32, no. 6, Dec. 2016.